



Ergodic versus diffusive decoherence in mesoscopic devices

Thibaut Capron,¹ Christophe Texier,^{2,3} Gilles Montambaux,³ Dominique Mailly,⁴
Andreas D. Wieck,⁵ and Laurent Saminadayer^{1,6,7,*}

¹*Institut Néel, B.P. 166, 38042 Grenoble Cedex 09, France*

²*Université Paris Sud, CNRS, LPTMS, UMR 8626, Bâtiment 100, F-91405 Orsay, France*

³*Université Paris Sud, CNRS, LPS, UMR 8502, Bâtiment 510, F-91405 Orsay, France*

⁴*Laboratoire de Photonique et Nanostructures, route de Nozay, 91460 Marcoussis, France*

⁵*Lehrstuhl für Angewandte Festkörperphysik, Ruhr-Universität, Universitätsstraße 150, 44780 Bochum, Germany*

⁶*Université Joseph Fourier, B.P. 53, 38041 Grenoble Cedex 09, France*

⁷*Institut Universitaire de France, 103 boulevard Saint-Michel, 75005 Paris, France*

(Received 25 June 2012; revised manuscript received 8 November 2012; published 29 January 2013)

We report on the measurement of phase coherence length in a high-mobility two-dimensional electron gas patterned in two different geometries, a wire and a ring. The phase coherence length is extracted both from the weak localization correction in long wires and from the amplitude of the Aharonov-Bohm oscillations in a single ring, in a low-temperature regime when decoherence is dominated by electronic interactions. We show that these two measurements lead to different phase coherence lengths, namely $L_{\phi}^{\text{wire}} \propto T^{-1/3}$ and $L_{\phi}^{\text{ring}} \propto T^{-1/2}$. This difference reflects the fact that the electrons winding around the ring necessarily explore the whole sample (ergodic trajectories), while in a long wire the electrons lose their phase coherence before reaching the edges of the sample (diffusive regime).

DOI: [10.1103/PhysRevB.87.041307](https://doi.org/10.1103/PhysRevB.87.041307)

PACS number(s): 73.23.-b, 03.65.Ta, 75.20.Hr, 72.70.+m

Understanding the mechanisms of decoherence is a major issue in mesoscopic physics, as it limits the existence of electronic interference effects.^{1,2} The experimental determination of this quantity is thus of crucial importance. At relatively high temperature (typically above 1 K), the electronic phase coherence is limited by electron-phonon collisions.³ Contrarily, at low temperatures, it is governed by electron-electron interactions: The measurement of the phase coherence time $\tau_{\phi}(T)$ thus provides an important check of the theoretical models concerning these electronic interactions in metals^{4,5} and a probe for studying the fundamental question of the interplay between interaction and disorder.

As it is well known that in diffusive conductors the temperature dependence $\tau_{\phi}(T)$ depends on space dimensionality d ; it has long been assumed that it depends *only* on d . However, it turns out that the situation is richer in quasi-one-dimensional systems ($d = 1$), where decoherence results mostly from processes involving small energy exchange between electrons, therefore implying long length scales. Indeed it has been shown in a pioneering work⁶ that in this case, the decoherence mechanism can be seen as the result of the interaction between one electron and the fluctuating electric field due to other electrons; the random phase accumulated by an electron along its diffusive trajectory increases with time with a characteristic time $\tau_{\phi}^{\text{wire}}(T) \propto T^{-2/3}$. Implicitly this analysis is valid for a infinite quasi-1D wire where diffusion is not limited in space. It has successfully explained many experiments on quasi-1D metallic or semiconducting wires.

In contrast, in a wire of finite length L , long diffusive trajectories are obviously limited at this length scale L , which must necessarily affect the decoherence mechanism. This so-called *ergodic* regime is reached when the diffusion occurs over times longer than the Thouless time $\tau_D = L^2/D$, where D is the diffusion coefficient. The ergodic regime has not been explored experimentally in diffusive wires. One reason is that a transport experiment implies connecting the device to

external contacts; therefore it is hardly possible to investigate this ergodic regime in a mesoscopic wire.

An alternative and appropriate device consists of a ring in which the study of quantum oscillations in a magnetic field naturally provides a selection mechanism between diffusive and ergodic trajectories, because the harmonics of the oscillations necessarily involve winding (and therefore ergodic) trajectories. Several works⁷⁻¹¹ have predicted that the temperature dependence of the phase coherence time obtained from magnetoconductance (MC) oscillations behaves as $\tau_{\phi}^{\text{ring}}(T) \propto T^{-1}$ in contrast with the result for an infinite wire. The present work constitutes experimental evidence for such behavior in a single ring.

More precisely, the goal of this paper is to provide, through magnetotransport measurements, a detailed comparison of the phase coherence time measured in two different geometries, namely an infinitely long wire and a ring. In a long wire, interferences between time-reversed electronic trajectories give rise to the weak-localization (WL) correction to the *average* conductance. Its magnetic field dependence provides a measure of the phase coherence length $L_{\phi}^{\text{wire}} = \sqrt{D\tau_{\phi}^{\text{wire}}}$.^{2,12} In a single ring, the magnetic field reveals the *sample specific* interference pattern: It modulates the phase difference between electron paths in each arm, leading to the so-called Aharonov-Bohm (AB)¹³ periodic oscillations of the conductance.¹⁴ The amplitude of the AB oscillations, averaged over an appropriate range of magnetic field, is controlled by the phase coherence length $L_{\phi}^{\text{ring}} = \sqrt{D\tau_{\phi}^{\text{ring}}}$. In this Rapid Communication we present a quantitative analysis of the temperature dependence of L_{ϕ}^{ring} extracted from AB oscillations of a single weakly disordered ring. Our experimental analysis shows that the two phase coherence lengths L_{ϕ}^{ring} and L_{ϕ}^{wire} present two different temperature dependencies, thus confirming the importance of the diffusive versus ergodic nature of the electronic trajectories.¹⁵

Samples have been fabricated from high-mobility GaAs/AlGaAs heterostructures. These systems are intrinsically clean of magnetic impurities⁵ and thus provide a large phase coherence length only limited by electronic interactions at low temperature.¹⁷ Using electron beam lithography on polymethyl-methacrylate resist and shallow etching, we have patterned mesoscopic rings and arrays of wires in the two-dimensional electron gas (2DEG). In addition, a Hall bar allows the determination of the characteristics of the 2DEG: The electron density is $n_e = 1.56 \times 10^{11} \text{ cm}^{-2}$, the mobility $\mu_e = 3.1 \times 10^5 \text{ cm}^2/\text{Vs}$, and the elastic mean-free path $\ell_e^{(2\text{DEG})} = 2.13 \text{ }\mu\text{m}$, leading to a diffusion coefficient $D^{(2\text{DEG})} = 1700 \text{ cm}^2/\text{s}$.

Rings have a perimeter $L = 13.6 \text{ }\mu\text{m}$, a lithographic width $w_{\text{litho}}^{\text{ring}} = 740 \text{ nm}$, and are connected to large reservoirs, as presented in the inset of Fig. 2(b). Arrays of wires are composed of 20 wires in parallel (in order to suppress conductance fluctuations) of width $w_{\text{litho}}^{\text{wire}} = 800 \text{ nm}$ and length $L = 150 \text{ }\mu\text{m}$. Note that due to depletion effects, the real widths w^{ring} and w^{wire} are somehow smaller: It was shown in Ref. 17 for similar samples that depletion length is $\simeq 190 \text{ nm}$ leading to $w^{\text{wire}} \sim w^{\text{ring}} \sim 400 \text{ nm}$. Analysis of the MC of the wires shows that the mean-free path is close to the one of the 2DEG: $\ell_e \simeq \ell_e^{(2\text{DEG})}$. In the two geometries, we thus probe the diffusive quasi-1D regime ($L\phi \gg \ell_e, w$).

MC measurements are performed on the ring and the wires simultaneously, using a standard ac lock-in technique and a homemade ultralow-noise amplifier ($0.4 \text{ nV}/\sqrt{\text{Hz}}$) at room temperature.

We sweep the magnetic field perpendicularly to the sample on a span of $\pm 50 \text{ G}$ around zero field. The conductance of the arrays of wires increases with magnetic field as expected, due to the suppression of the weak-localization correction. We then fit the MC with the well-known expression^{2,12}

$$\Delta G = -\frac{2e^2}{h} \frac{1}{L} \left[\left(\frac{1}{L_{\phi}^{\text{wire}}} \right)^2 + \frac{1}{3} \left(\frac{ew_{*}^{\text{wire}}B}{\hbar} \right)^2 \right]^{-1/2}, \quad (1)$$

where w_* is an effective width accounting for flux cancellation effect [for a wire, $w_* = w$ if $\ell_e \ll w$ (Ref. 12) and $w_* \sim w\sqrt{w/\ell_e}$ if $\ell_e \gg w$ (Ref. 18)]. As shown in the inset of Fig. 1, we can extract L_{ϕ}^{wire} at several temperatures ranging from 52 mK to 1 K. The resulting temperature dependence of L_{ϕ}^{wire} is displayed in Fig. 1. In this temperature range, decoherence is dominated by electronic interactions, and the phase coherence length is given for quasi 1D diffusive samples by¹⁷

$$L_{\phi} = \sqrt{D\tau_{\phi}} = \sqrt{\frac{D}{aT^{\theta} + bT^2}}, \quad (2)$$

where, for a wire, $\theta = 2/3$ and the factor a is theoretically given by $D/a_{\text{theo}} = 2(m^*w^{\text{wire}}D^2/\pi k_B)^{2/3}$ with k_B the Boltzmann constant and m^* the effective mass of the electrons, whereas the adjustable parameter b takes into account interactions involving high-energy transfers.^{6,17,19,21} As shown on Fig. 1, $L_{\phi}^{\text{wire}}(T)$ is well described by Eq. (2), setting a_{exp} as a fitting parameter. A quantitative comparison of a_{exp} and a_{theo} for similar wires has been provided in Ref. 17 and has shown that the analysis of the WL leads to a reliable determination of L_{ϕ}^{wire} ; we will not elaborate more on this point since the present analysis does not rely on it.

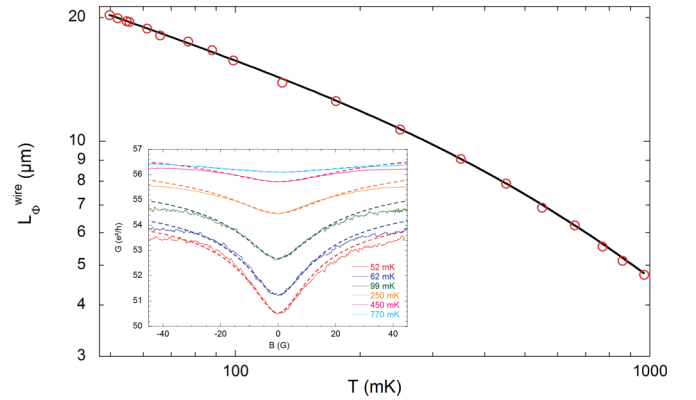


FIG. 1. (Color online) Phase coherence length L_{ϕ}^{wire} as a function of temperature, extracted from weak-localization measurements. The solid line shows the theoretical fit to Eq. (2), using $\theta = 2/3$. Inset: Magnetoconductance of the wires measured at several temperatures. Dashed lines represent the fits to Eq. (1).

The magnetoconductance measured in the ring presents periodic oscillations. After subtraction of a smooth background component, we obtain the characteristic Aharonov-Bohm oscillations shown in Fig. 2(a). These oscillations are Φ_0 periodic with the magnetic flux, where $\Phi_0 = h/e$. This corresponds to a field periodicity $B_0 = \Phi_0/(\pi r_0^2)$ with r_0 the mean radius of the ring. A Fourier transform of the signal is then performed using a rectangular window; this is presented in Fig. 2(b). A clear peak around $B_0 = 2.7 \text{ G}$ appears in the spectrum. From this value, we can extract $r_0 = 2.17 \text{ }\mu\text{m}$, in excellent agreement with the lithographic radius $r_0 = 2.13 \text{ }\mu\text{m}$.

In the following, we detail the procedure used to extract the amplitude of the AB oscillations. As the width of the arms of the ring is finite, all electron trajectories lying between the inner radius r_1 and the outer radius r_2 of the ring can participate in the oscillations. In addition, due to depletion inherent in the fabrication process (etching), the inner and outer radii are not the lithographic ones and the effective width of the arms of the ring w^{ring} is smaller than $w_{\text{litho}}^{\text{ring}}$. We observe a broadening of the Fourier peak between $1/B_2$ and $1/B_1$ [dashed lines in Fig. 2(b)] corresponding to $B_1 = \Phi_0/(\pi r_1^2)$ and $B_2 = \Phi_0/(\pi r_2^2)$. From these results, we can extract the effective width $w^{\text{ring}} = r_2 - r_1 = 360 \text{ nm}$; it corresponds to a depletion length of 190 nm , in accordance with the value reported elsewhere using another method on similar samples.¹⁷ The conductance oscillations are Fourier transformed over a window $[-50 \text{ G}, +50 \text{ G}]$ (larger than the correlation field estimated to be $B_c \sim 8 \text{ G}$). We clearly identify a peak corresponding to the AB Φ_0 -periodic oscillations (Fig. 2): In this case the AB amplitude is given by integrating this peak as $\delta G_{\text{AB}}^2 \propto \int_{\text{peak}} h/e dK \delta \bar{G}(K)^2$ where $\delta \bar{G}(K)$ is the Fourier transform plotted in Fig. 2(b). Theoretically, we expect that, for $L_{\phi}^{\text{ring}} \ll L$, δG_{AB} depends on L_{ϕ}^{ring} as¹⁴

$$\delta G_{\text{AB}} \simeq C \frac{e^2}{h} \frac{L_T}{L} \left(\frac{L_{\phi}^{\text{ring}}}{L} \right)^{\eta} e^{-L/2L_{\phi}^{\text{ring}}}, \quad (3)$$

where $L_T = \sqrt{\hbar D/k_B T}$ is the thermal length, L the perimeter of the ring, and C a constant of order 1. The exponent η depends on the nature of the contacts. If the ring is isolated it is equal to

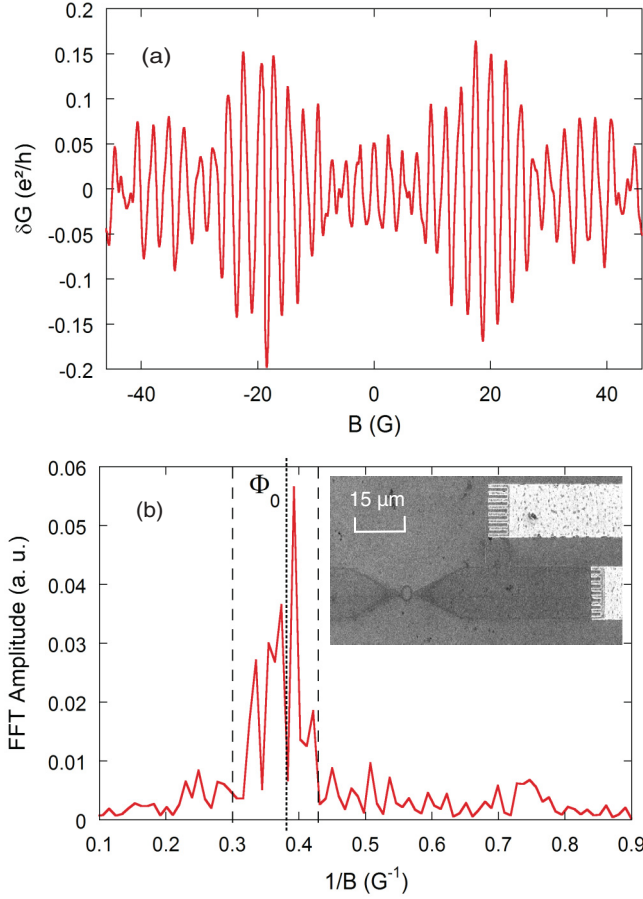


FIG. 2. (Color online) (a) Magnetoconductance δG of the ring measured at 55 mK, after subtraction of a smooth background signal. (b) Fourier transform $\delta \tilde{G}$ of the signal showing the $\Phi_0 = h/e$ periodicity at B_0 (dotted line). The width of the main peak is represented by the dashed lines and corresponds to the values $1/B_{1,2}$ for the inner and outer $r_{1,2}$ radii of the ring. Inset: Scanning electron microscope image of the ring.

$\eta = 1/3$.^{8,9,22} We now justify that this value is appropriate in our samples. The 2D large contacts are connected to the ring through relatively narrow constrictions of width of the same order than w^{ring} . Because the motion is ballistic at the scale of the contact (since $\ell_e > w^{\text{ring}}$), forward scattering should be favored for an electron winding inside the ring; i.e., the probability to exit should be diminished, compared to the diffusive contact with $\ell_e \ll w^{\text{ring}}$. Note however that the value of η will not affect strongly the fitting procedure for L_Φ^{ring} .

From the experimental data we can extract the phase coherence length in the ring L_Φ^{ring} as a function of temperature. Note that Eq. (3) is strictly valid only in the regime where $L_\Phi < \pi r_0$, the length of one arm of the ring. Indeed, in the opposite case $L_\Phi > \pi r_0$, electrons may explore the contacts with a high probability, which affects the decoherence and strongly modifies the L_Φ dependence of the AB amplitude:^{9,22,23} For this reason, our analysis only holds above $T \simeq 300$ mK.

A direct comparison between $L_\Phi^{\text{wire}}(T)$ and $L_\Phi^{\text{ring}}(T)$ is presented in Fig. 3. We observe that the two phase coherence lengths differ both in *absolute value* and in *temperature dependence*. By fitting the data we obtain $L_\Phi^{\text{wire}} \propto T^{-0.33 \pm 0.01}$

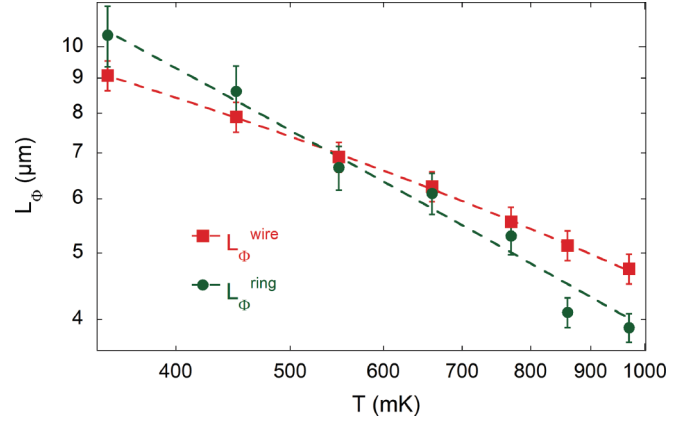


FIG. 3. (Color online) Phase coherence lengths obtained in a wire, L_Φ^{wire} , and in a ring, L_Φ^{ring} , as a function of temperature. The dashed lines show the theoretical fit obtained with Eq. (2).

for the wire and $L_\Phi^{\text{ring}} \propto T^{-0.49 \pm 0.09}$ for the ring.^{24,25} These exponents are in perfect agreement with the theoretical predictions $L_\Phi^{\text{wire}} \propto T^{-1/3}$ ⁶ and $L_\Phi^{\text{ring}} \propto T^{-1/2}$ (Refs. 7–9).

We now recall simple arguments to understand the different exponents.^{7–9,16} In Ref. 6, it is argued that decoherence results from the randomization of the phase of a given electron by the fluctuating electric field created by other electrons. Within this picture an electron receives a phase $\Phi(t) \sim \int_0^t d\tau V(\tau)$ from the electric potential whose fluctuations are characterized by the fluctuation-dissipation theorem $\int d\tau \langle V(\tau)V(0) \rangle \sim e^2 T \mathcal{R}_t$, where \mathcal{R}_t is the resistance of the part of the sample probed by the electron during a time scale t . It can be written $\mathcal{R}_t \sim x(t)/s\sigma_0$, where s is the section of the wire, σ_0 the Drude conductivity, and $x(t)$ the distance covered by the electron. The electronic phase presents a behavior with time given by $\langle \Phi(t)^2 \rangle \sim \int_0^t d\tau \int_0^t d\tau' \langle V(\tau)V(\tau') \rangle \sim e^2 T t x(t)/s\sigma_0$. In a long wire, the motion is of diffusive nature, $x(t) \sim \sqrt{Dt}$, leading to the phase diffusion $\langle \Phi(t)^2 \rangle \sim e^2 T t^{3/2} \sqrt{D}/s\sigma_0$. We extract the relevant time scale by writing $\langle \Phi(t)^2 \rangle \sim (t/\tau_\Phi^{\text{wire}})^{3/2}$ with $\tau_\Phi^{\text{wire}} \propto T^{-2/3}$. In a ring, the winding trajectories are ergodic and the length $x(t)$ is simply the size of the system; we thus obtain the behavior $\langle \Phi(t)^2 \rangle \sim e^2 T t L/s\sigma_0 \sim t/\tau_\Phi^{\text{ring}}$, leading to the time scale $\tau_\Phi^{\text{ring}} \propto T^{-1}$. We may write the relation between the two times as $\tau_\Phi^{\text{ring}} \sim (\tau_\Phi^{\text{wire}})^{3/2}/(\tau_D)^{1/2}$, where $\tau_D = L^2/D$ is the Thouless time. The precise dimensionless factor has been obtained by a careful analysis of the MC curve in Refs. 8,9,16, and 22:

$$L_\Phi^{\text{ring}} = \frac{2^{9/4} (L_\Phi^{\text{wire}})^{3/2}}{\pi L^{1/2}}, \quad (4)$$

where $L_\Phi = \sqrt{D\tau_\Phi}$. In Fig. 4 we check that $L_\Phi^{\text{ring}}(T)$ and $L_\Phi^{\text{wire}}(T)$ extracted from the experiment obey relation (4) with a very good accuracy. The experimental verification of this relation definitely proves that the two temperature dependencies of $L_\Phi(T)$ for the wire and for the ring emerge from the same mechanism described in a coherent picture.^{7–9}

Finally we comment on an issue which has been debated in the past:^{8,26} For a given geometry, are the phase coherence length obtained from weak localization (WL) and conductance fluctuations (CF) identical? In Ref. 16, the measurement of the WL of a large array of rings has led to $L_\Phi^{\text{ring,WL}} \propto T^{-1/2}$.

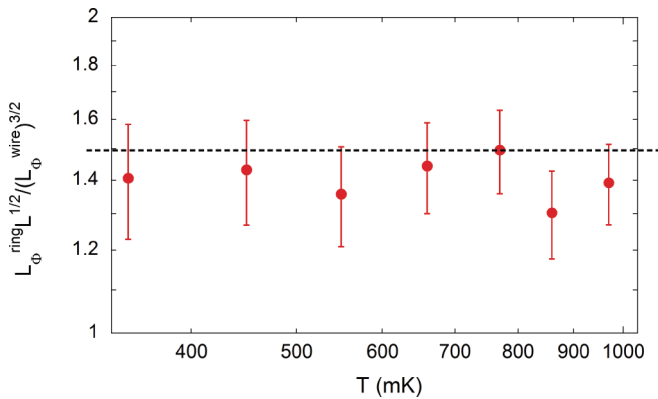


FIG. 4. (Color online) Experimental test of Eq. (4), from the phase coherence lengths extracted from AB oscillations of the ring and WL of the wire. The dotted line corresponds to $2^{9/4}/\pi \simeq 1.514$.

This corresponds *quantitatively* to $L_{\phi}^{\text{ring,CF}} \propto T^{-1/2}$ obtained here. These two measurements therefore give an experimental demonstration that the phase coherence lengths extracted from WL and CF are indeed the same.²⁷

In conclusion, we have measured the phase coherence length L_{ϕ} in samples etched in 2DEG of two different geometries by analyzing quantum corrections to the magneto-

conductance. We have been able to extract the temperature dependence of the phase coherence length from the AB harmonics of a single diffusive ring. The phase coherence length obtained from this method presents the behavior $L_{\phi}^{\text{ring}} \propto T^{-1/2}$ different from the one obtained from the MC of a long wire, $L_{\phi}^{\text{wire}} \propto T^{-1/3}$. This demonstration of the geometrical sensitivity of the decoherence process by electronic interactions emphasizes the very precise understanding of the role of electronic interactions on low temperature phase coherent properties of metals. In the present work, we have been able to investigate ergodic trajectories in a nonergodic temperature regime, $T > 1/\tau_{\phi} > 1/\tau_D$, thanks to the selection of winding trajectories by the magnetic field. An experimental exploration of lower temperature is still desired: When $\tau_{\phi} > \tau_D$, quantum interferences involve large-scale properties which affect the decoherence process.⁹ The investigation of the 0D regime,^{10,11,30} $1/T > \tau_D$, still remains a challenging issue.

We acknowledge helpful discussions with H. Bouchiat, M. Ferrier, T. Ludwig, A. D. Mirlin, M. Treiber, J. von Delft, and O. M. Yevtushenko. This work has been supported by the European Commission FP6 NMP-3 project 505457-1 ‘‘Ultra 1D’’ and the *Agence Nationale de la Recherche* under the grant ANR PNano ‘‘QuSpin.’’ A.D.W. acknowledges gratefully support from DFG SPP1285 and BMBF QuaHL-Rep 01BQ1035.

*saminadayar@grenoble.cnrs.fr

¹Y. Imry, *Introduction to Mesoscopic Physics* (Oxford University Press, 1997).

²E. Akkermans and G. Montambaux, *Mesoscopic Physics of Electrons and Photons* (Cambridge University Press, Cambridge, 2007).

³S. Chakravarty and A. Schmid, *Phys. Rep.* **140**, 193 (1986).

⁴F. Pierre, A. B. Gougam, A. Anthore, H. Pothier, D. Esteve, and N. O. Birge, *Phys. Rev. B* **68**, 085413 (2003).

⁵L. Saminadayar, P. Mohanty, R. A. Webb, P. Degiovanni, and C. Bäuerle, *Physica E* **40**, 12 (2007).

⁶B. L. Altshuler, A. G. Aronov, and D. E. Khmel'nitsky, *J. Phys. C: Solid State Phys.* **15**, 7367 (1982).

⁷T. Ludwig and A. D. Mirlin, *Phys. Rev. B* **69**, 193306 (2004).

⁸C. Texier and G. Montambaux, *Phys. Rev. B* **72**, 115327 (2005).

⁹C. Texier, P. Delplace, and G. Montambaux, *Phys. Rev. B* **80**, 205413 (2009).

¹⁰M. Treiber, O. M. Yevtushenko, F. Marquardt, J. von Delft, and I. V. Lerner, *Phys. Rev. B* **80**, 201305 (2009).

¹¹M. Treiber, C. Texier, O. M. Yevtushenko, J. von Delft, and I. V. Lerner, *Phys. Rev. B* **84**, 054204 (2011).

¹²B. L. Al'tshuler and A. G. Aronov, *JETP Lett.* **33**, 499 (1981) [*Pis'ma Zh. Eksp. Teor. Fiz.* **33**, 515 (1981)].

¹³The AB effect [Y. Aharonov and D. Bohm, *Phys. Rev.* **115**, 485 (1959)] was in fact proposed earlier in W. Ehrenberg and R. E. Siday, *Proc. Phys. Soc. (London)* **B 62**, 8 (1949).

¹⁴S. Washburn and R. A. Webb, *Adv. Phys.* **35**, 375 (1986).

¹⁵Different temperature-dependent phase coherent lengths have been extracted in the recent analysis of the WL in samples made of a large number (10^6) of rings arranged to form a grid (Ref. 16).

¹⁶M. Ferrier, A. C. H. Rowe, S. Gueron, H. Bouchiat, C. Texier, and G. Montambaux, *Phys. Rev. Lett.* **100**, 146802 (2008).

¹⁷Y. Niimi, Y. Baines, T. Capron, D. Mailly, F.-Y. Lo, A. D. Wieck, T. Meunier, L. Saminadayar, and C. Bäuerle, *Phys. Rev. Lett.* **102**, 226801 (2009); *Phys. Rev. B* **81**, 245306 (2010).

¹⁸V. K. Dugaev and D. E. Khmel'nitskiĭ, *JETP* **59**, 1038 (1984) [*Zh. Eksp. Teor. Fiz.* **86**, 1784 (1984)]; C. W. J. Beenakker and H. Van Houten, *Phys. Rev. B* **38**, 3232 (1988); H. Van Houten *et al.*, *Surf. Sci.* **196**, 144 (1988).

¹⁹In Ref. 20, the study of the crossover between diffusive and ballistic regimes in 2D samples has shown that the decoherence rate is given by the addition of a term $\propto T$ (2D-diffusive) and a term $\propto T^2$ (ballistic) (Refs. 6 and 21). We assume that diffusive and ballistic rates can also be added in the quasi-1D geometry.

²⁰B. N. Narozhny, G. Zala, and I. L. Aleiner, *Phys. Rev. B* **65**, 180202 (2002).

²¹H. Fukuyama and E. Abrahams, *Phys. Rev. B* **27**, 5976 (1983).

²²C. Texier, *Phys. Rev. B* **76**, 153312 (2007).

²³V. Chandrasekhar, P. Santhanam, and D. E. Prober, *Phys. Rev. B* **44**, 11203 (1991); K. Kobayashi, H. Aikawa, S. Katsumoto, and Y. Iye, *J. Phys. Soc. Jpn.* **71**, 2094 (2002).

²⁴Measurements consistent with $L_{\phi} \propto T^{-1/2}$ in similar samples were mentioned in L. Angers, E. Zakka-Bajjani, R. Deblock, S. Guéron, H. Bouchiat, A. Cavanna, U. Gennser, and M. Polianski, *Phys. Rev. B* **75**, 115309 (2007).

²⁵Note that $L_{\phi} \propto T^{-1}$ was extracted from AB oscillations of ballistic rings in A. E. Hansen, A. Kristensen, S. Pedersen, C. B. Sørensen, and P. E. Lindelof, *Phys. Rev. B* **64**, 045327 (2001).

²⁶Ya. M. Blanter, *Phys. Rev. B* **54**, 12807 (1996); I. L. Aleiner and Ya. M. Blanter, *ibid.* **65**, 115317 (2002).

²⁷The relation between AB oscillations (CF) and Altshuler-Aronov-Spivak oscillations (WL) (Ref. 28) has been verified as a function of the sample size at a *fixed* temperature in Ref. 29.

²⁸B. L. Al'tshuler, A. G. Aronov, and B. A. Spivak, JETP Lett. **34**, 94 (1981).

²⁹F. Schopfer, F. Mallet, D. Mailly, C. Texier, G. Montambaux, C. Bäuerle, and L. Saminadayar, *Phys. Rev. Lett.* **98**, 026807 (2007).

³⁰U. Sivan, Y. Imry, and A. G. Aronov, *Europhys. Lett.* **28**, 115 (1994).